A Histopathologic Evaluation of the Plasma Skin Regeneration System (PSR) Versus a Standard Carbon Dioxide Resurfacing Laser in an Animal Model

R. Fitzpatrick, MD,[1]* E. Bernstein, MD,[2] S. Iyer, MD,[3] D. Brown, PhD,[2] P. Andrews,[4] and K. Penny, MSc[4]

[1]*La Jolla Cosmetic Surgery Centre, San Diego, California*
[2]*DakDak, LLC, Elkins Park, Pennsylvania*
[3]*New York Dermatology Group, New York, New York*
[4]*Rhytec Ltd, UK*

Background and Objectives: A variety of high energy, pulsed, and scanned carbon dioxide lasers are available to perform cutaneous resurfacing. Rhytec has developed a device for skin regeneration that utilizes energy delivered via a burst of nitrogen plasma. This study was undertaken to benchmark the energy outputs of the plasma skin regeneration device as compared to an ultra-short pulsed carbon dioxide laser (the control device). The two systems were compared for time to complete healing, and the healing response post-treatment.

Materials and Methods: Three Yucatan mini-pigs were utilized for this study. Following anesthesia, five experimental sites were marked along the skin atop the psoas muscle on each side of the spine. Treatment was applied using either the plasma skin regeneration system or the carbon dioxide laser, with one site remaining untreated as a control. Biopsies were taken from all treatment sites 0, 2, 7, 14, 30, and 60 days following treatment and processed to hematoxylin-eosin staining. Histopathologic examination was performed by observers blinded as to the treatment conditions.

Results: Skin treated with the plasma skin regeneration device showed a wider range of tissue effects across the energy settings used as compared to the laser treatment. All treatment sites had clinically regenerated epidermis by 7 days after treatment, with active cellular response below the D/E junction noted at the day 30 time-point at energies ranging from 2 to 4 J.

Conclusion: The Rhytec PSR system provides an attractive alternative to standard CO_2 laser with good remodeling of tissue architecture. Epidermis regenerated after PSR treatment shows a smoother surface profile than adjacent untreated tissue. Lasers Surg. Med. 40:93–99, 2008.

Key words: PSR; regeneration/resurfacing; plasma; CO_2; remodeling

INTRODUCTION

Short-pulsed, high energy, rapidly scanned carbon dioxide (CO_2) laser has been used for many years in a wide range of applications including removal of superficial skin lesions and skin resurfacing [1]. However, efficacy and safety require strict adherence to set guidelines. Lasers can ablate epidermis with minimal damage to the underlying dermis. The wavelength of 10,600 nm emitted by the CO_2 laser is specifically absorbed by water contained within all the cells of the skin. Following absorption, the light energy is converted into heat energy by excitation of the water molecules. The thermal energy leads to local tissue destruction. Reducing the length of the laser pulse minimizes thermal injury to adjacent tissues by reducing heat conduction away from the target tissue.

A new modality known as the Plasma Skin Regeneration System (PSR) allows precise and also rapid heating of tissue so that all or part of the epidermis becomes nonviable and there is controlled thermal modification to the underlying dermis with minimal thermal injury to surrounding tissues. The zone of thermal injury is thought to be significantly less than the CO_2 laser [2]. Ultra high frequency (UHF) energy from the generator converts nitrogen gas into plasma within the hand-piece. Plasma is the fourth state of matter (solid, liquid, and gas being the other three), in which electrons are stripped from atoms to form ionized gas. The plasma emerges from the nozzle at the distal end of the hand-piece and is directed onto the skin to be treated. Rapid heating of the skin occurs as the excited gas gives up energy to the skin.

Through the controlled application of UHF energy to a flow of inert nitrogen gas, and the essentially instantaneous generation of plasma, individual plasma pulses are produced which give consistent tissue effects. Adjustment of the UHF power and UHF pulse width (range 5–16 milliseconds) by the generator enables control of tissue effects by altering the amount of energy delivered to tissue per pulse. In practice, the energy per pulse is adjustable by the user from 1 to 4 J, in 0.1 J increments. This allows the user to select the appropriate energy level in relation to the effect he wishes to achieve, ranging from minimal thermal damage to desiccation of the epidermal layer.

*Correspondence to: R. Fitzpatrick, MD, SkinMedica, Inc., 5909 Sea Lion Place Suite E, Carlsbad, CA 92010.
E-mail: aandrews@skinmedica.com
Accepted 24 August 2007
Published online in Wiley InterScience (www.interscience.wiley.com).
DOI 10.1002/lsm.20547

This spectrum of effect is achieved by efficiently transferring energy to the skin via thermal conduction. As PSR is not dependant upon a chromophore in the skin to mediate energy absorption, a unique thermal profile is observed histologically, resulting in an even delivery of energy that is characterized by two distinct zones of effect (Fig. 1). The first zone noted is a zone of thermal damage (ZTD), which can extend from the upper epidermis to the papillary dermis, depending upon energy setting. Cells in this zone are non-viable, and shed in the subsequent post-treatment phase. The second zone underlying the ZTD is a zone of thermal modification (ZTM), wherein the cells are denatured, yet remain viable. In the post-treatment phase, this zone is a site of intense remodeling, with fibroblast activity noted histologically in the post-treatment phase, resulting in new epidermal and dermal architecture being generated.

The presence of inert nitrogen flowing after the plasma impact suppresses oxidization effects and the energy delivery profile does not produce explosive or vaporization effects associated with ablative lasers. In practice this is characterized by the absence of char formation on the treated skin, with the epidermal layer remaining intact.

OBJECTIVES

The objective of the investigation was to compare the ultra-short pulse-duration carbon dioxide laser and the PSR device under normal conditions of use in the performance of skin resurfacing procedures. The investigation sought to compare the PSR device and the CO_2 laser in terms of tissue effect and post-procedural healing, and to analyze the tissue response to the plasma pulses over time.

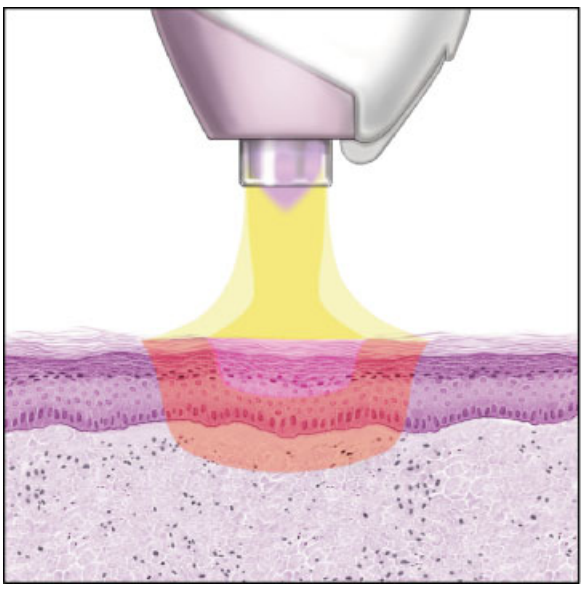

Fig. 1. The two distinct zones of effect produced by the plasma. Inner/pink: Zone of Thermal Damage (ZTD) Outer/red: Zone of Thermal Modification (ZTM).

MATERIALS AND METHODS

Experimental Devices

PSR. The generator provides a stable high frequency source for the generation of RF energy. The precise control of the UHF energy from the PSR system allows plasma to be generated from a stream of nitrogen gas. This plasma consists of highly excited ionized gas. The visible plume that emerges from the hand-piece is known as a Lewis Rayleigh Afterglow, characterized by a yellowish light that is emitted as excited nitrogen molecules relax from the N2(B) to the N2(A) energy state. In a low-pressure chamber, the Lewis-Rayleigh Afterglow can visibly persist for many minutes. However, under the atmospheric conditions of use for PSR the excited nitrogen disperses quickly on mixing with air.

Directing the plasma onto a solid such as skin results in rapid relaxation of the excited nitrogen because molecular collisions are far more numerous. As the pulsed plasma hits the tissue, it imparts energy to the surface. The gas flow rate affects energy delivery to the target tissue and is accurately regulated. The power and duration of each UHF pulse has a great influence on the energy imparted to the skin. The instrument does not contact the tissue but is held approximately 5 mm from the skin's surface. With increased "stand-offs" the energy delivered to tissue is reduced.

The UHF energy is continuously monitored within the generator such that a cut-off would occur with equipment malfunction. There is no direct means for radio frequency (RF) transfer from the system to a patient. The generator is powered from a conventional ISA wall socket. The user interface consists of a large character illuminated display giving clear readings of energy per plasma pulse and the pulse repetition rate.

A lightweight arm supports the cabling and gas feed tube and leads to the broad pen-shaped hand-piece housing the plasma chamber. A transparent plasma nozzle enhances the visibility of target tissue. This and the resonator are disposable, due to the physical erosion of these components over time. Plasma strikes are applied to the target tissue with contiguous footprints (multiple small areas of treatment that join to form a larger treatment area).

The product has been designed to meet the requirements of EN 60601 (including EMC) and California short-term exposure limits for nitrogen dioxide production.

Carbon dioxide laser. An UltraPulse 5000C carbon dioxide laser (Coherent Medical Group, Palo Alto, CA) was used as the Control device. The UltraPulse can deliver from single 600-microseconds to 1-millisecond pulses with peak energies of 500 mJ. The energy fluence that is delivered in each pulse is greater than the 2–5 J/cm^2 ablation threshold of skin. The target tissue (water) is vaporized faster than the heat can be conducted to adjacent tissue, resulting in a defined zone of thermal damage that is significantly less than that seen with continuous wave CO_2 lasers, where as much as 1 mm of thermal damage around the treatment site can be produced.

The UltraPulse is equipped with a computerized pattern generator (CPG). The CPG hand-piece allows 2.25-mm

spots to be delivered using various geometric patterns and energies. A large square pattern can be employed that allows rapid treatment of large areas. A rectangular pattern (59) was used in the study. The density of the pattern can be low (i.e., non-overlapping spots) or high (i.e., 10–60% overlapping spots). The CPG is typically used at 300 mJ and 60 W. The UltraPulse will typically ablate 20–30 μm of tissue per pass, and up to 100 μm, but this is dependent upon the density employed [3,4].

Laser and PSR treatment. The investigation was performed in a controlled laboratory environment according to the GLP guidelines (Perry Scientific Inc., San Diego, CA). Three Yucatan Mini pigs, weighing between 20 and 30 kgs, purchased from an approved source, were used for this study. This species was chosen as the model in this investigation for two reasons: their skin bears a close similarity to that of humans, and as the study was being conducted over a 60 day timeframe, minimal growth was required in order to avoid untoward changes in the treatment sites. Pigs were kept in an environmentally controlled environment and given food and water ad libitim. Prior to treatment, pigs were anesthetized and the skin was cleansed with soap and water, and then dried. Excess hair was removed with clippers prior to treatment. Using a template, five experimental sites measuring 3.5 cm×3.5 cm were identified and marked along the psoas muscle ridges on each side of the spine. Each experimental site was at least 2 cm remote from the adjacent site and all sites were at least 2 cm from the spine dorsal midline. Figure 2 demonstrates the treatment pattern and the biopsy sites for each experimental site. Treatment was then applied to each of the sites, according to the experimental plan, with one of the following regimes:

(1) Laser, low fluence, 150 mJ per pulse, pattern sequence 59, density 6
(2) Laser, medium fluence, 300 mJ per pulse, pattern sequence 59, density 5
(3) Laser, high fluence, 300 mJ per pulse, pattern sequence 59, density 9
(4) PSR, 1 J, shortest pulse time @ 1.5 Hz

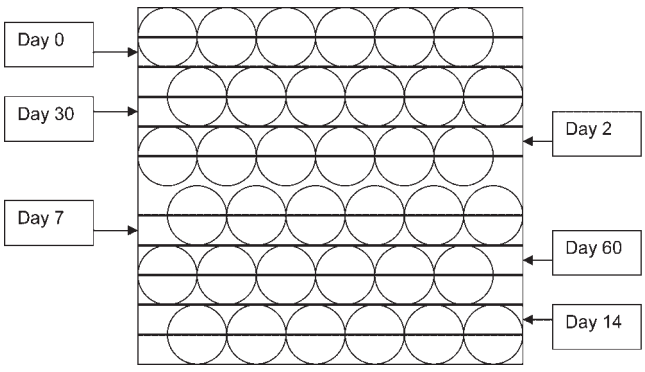

Fig. 2. The treatment pattern and the biopsy sites for each experimental site.

(5) PSR, 2 J, shortest pulse time @ 1.5 Hz
(6) PSR, 2.5 J, shortest pulse time @ 1.5 Hz
(7) PSR, 3 J, shortest pulse time @ 1.5 Hz
(8) PSR, 3.5 J, shortest pulse time @ 1.5 Hz
(9) PSR, 4 J, shortest pulse time @ 1.5 Hz
(10) No treatment as control tissue

The UltraPulse 5000C was set at 60 W power, 200 Hz repetition rate.

Two nozzle types were used with the PSR system: nozzle 1 was the standard 6 mm diameter nozzle, whereas nozzle 2 was a custom, 2 mm narrow nozzle under evaluation. For the first pig, treatment consisted of a single pass in each site. For the second pig, treatment consisted of two passes in the PSR sites and a single pass in the laser sites. The double pass with the PSR device was performed in order to facilitate characterization of the thermal effect created in the skin by multiple passes. In the third animal, treatment consisted of a single pass in each site, with the narrow nozzle device employed on the PSR system. This allowed characterization of the thermal effect created with this device and allowed comparison of effect with the standard PSR nozzle. None of the treatment sites on any of the animals were wiped to remove the treated epidermis (Fig. 3).

Immediately following the completion of all treatments and starting with the first treatment site, a strip biopsy approximately 3 mm wide and deep to the muscle layer was excised and placed into 10% neutral-buffered formal saline and fixed for no less than 48 hours. The biopsy defect was then sutured closed. Because of the large quantity of tissue being excised in this manner, the method of obtaining biopsies was changed from day 14, with a move to 4 mm punch biopsies occurring. Digital photographs of the treatment sites were taken at the time of treatment and at each subsequent biopsy session, to provide a visual record of the healing process.

Once all the biopsies had been excised, the wounds were covered with petroleum jelly and Jelonet paraffin gauze, followed by non-filamented packing swabs held in place with self-adhesive dressing tape and an elasticized bandage. This was then protected from disturbance by the use of a jacket strapped to the torso of the animal. The animals were recovered from anesthesia and returned to the animal accommodation.

On days 2, 7, 14, 30, and 60 post-treatment, the pigs were pre-medicated and anesthetized in the manner previously described, the dressings removed, macroscopic assessment of the experimental sites recorded, the experimental sites re-marked, and further biopsies excised from each experimental site. The experimental sites were then re-dressed, the animals recovered from anesthetic and returned to the animal accommodation.

Evaluation of biopsy samples. Biopsy samples were fixed in formalin, sectioned, and stained with hematoxylin-eosin for histopathologic evaluation, and 4-micron sections were obtained. Thin sections were visualized using an Olympus BX40 microscope (Olympus, Tokyo, Japan) using

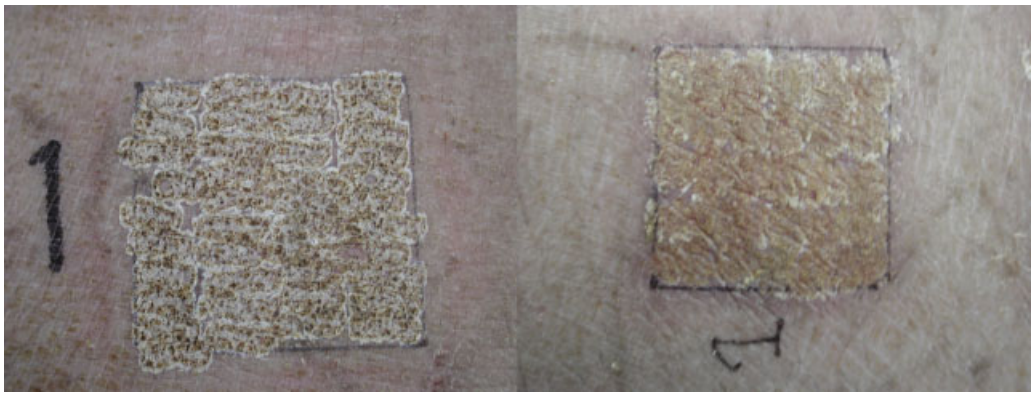

Fig. 3. High fluence CO_2 laser (**left**) and 4 J, single pass PSR (**right**) immediately post-treatment.

an Olympus 4× Plan objective. Digital images were acquired with the Kodak DCS 420c digital camera (Kodak, Rochester, NY) attached directly to the microscope. The images are ported to Photoshop 4.0 (Adobe, Mountain View, CA) using a PowerMac 8500 computer (Apple Computers, Cupertino, CA), and then transported to the image analysis software, NIH image 1.59 (National Institutes of Health, Bethesda, MD) for determination of the average thickness of thermal damage. Three biopsy specimens were harvested at each PSR or laser energy site. Three tissue sections were analyzed for each biopsy specimen, each section separated from one another by at least 16 microns in the tissue block. All photographs were numerically coded before observation. All coded biopsies were read by three observers for epidermal necrosis immediately post-treatment, intact epidermis post-treatment, and inflammatory infiltrate post-treatment.

Epidermal necrosis. Epidermal necrosis on the day of treatment was graded on a 0–5 scoring scale, with 0 representing no necrosis and 5 representing complete necrosis of the epidermis in a histopathological section. Specifically: 0 = no necrosis, 1 = sparse necrosis throughout the epidermis, 2 = up to 25% epidermal necrosis; necrosis not confluent along dermal/epidermal (D/E) junction, 3 = up to 50% epidermal necrosis; necrosis confluent along D/E junction, 4 = up to 75% epidermal necrosis; necrosis not only confluent along D/E junction, but also necrosis extends throughout the depth of the epidermis in some (not all) areas, 5 = complete epidermal necrosis. The percentage of the epidermis that was intact or present following treatment was evaluated on all evaluation days post-treatment: days 0, 2, 7, 14, 30, and 60 post-treatment. The degree of inflammation was also evaluated for all measur–ed time-points post-treatment.

Inflammatory infiltrate. Inflammation was graded on a 0–5 scoring scale. Evaluation was performed all time points (days 0, 2, 7, 14, 30, and 60). A score of 0 = no inflammation, 1 = sparse inflammation in the papillary dermis with no inflammation in the reticular dermis, 2 = inflammation found in up to 25% of the papillary dermis or sparse inflammation found in the reticular dermis, 3 = inflammation found in up to 50% of the papillary dermis or sparse inflammation in the reticular dermis, 4 = inflammation found in up to 75% of the papillary dermis or inflammation found in up to 50% of the reticular dermis, and 5 = inflammation found in up to 100% of the papillary dermis or up to 100% in the reticular dermis.

An *F*-test was performed on all scores comparing the variation between observers' scores. An *F*-test returns the one-tailed probability that the variances in two arrays are not significantly different. A value of 1.0 equals identical arrays. In this analysis a variance of approximately 0.9 was found, indicating strong intra-observer correlation.

Zone of thermal damage. After treatment with the carbon dioxide laser or PSR device, a zone of thermally modified dermis appears below the dermal-epidermal junction. The depth of damage can be calculated using an image analysis program standardized to a micrometer mounted on a glass slide. A digital photograph to measure the depth of this zone was generated at the same level of magnification as the samples. The zone thickness as reported is the average of 10–15 measurements across three adjacent regions from a single tissue section (Table 1).

TABLE 1. Zone of Thermal Damage With Carbon Dioxide Laser and PSR Device

Zone of dermal thermal damage	Single pass (nozzle 1)	Double pass (nozzle 1)	Single pass (nozzle 2)	Average
Control	0.0	0.0	0.0	0.0
Low fluence	10.3	8.0	10.7	9.7
Med fluence	13.3	7.3	4.0	8.2
High fluence	37.7	26.7	36.0	33.4
1.0 J, PSR	0.0	0.0	0.0	—
2.0 J, PSR	9.0	21.0	7.0	—
2.5 J, PSR	8.0	11.0	6.0	—
3.0 J, PSR	7.0	6.0	7.0	—
3.5 J, PSR	8.0	9.0	7.0	—
4.0 J, PSR	13.0	11.0	8.0	—

Only laser-treated swine skin was averaged ($n = 3$). Zone thickness measurements are in microns.

Only the zone of thermal damage from the laser treatments was replicated in all the three pigs. Thus, an average from all three pigs was possible.

RESULTS

Zone of Thermal Damage

All three pigs had sites designated for three carbon dioxide laser treatments: low, medium, and high fluences. The results are reported as an average ± standard deviation (Fig. 4). The zone of thermal damage generated after laser treatment with a high fluence (33.4 ± 5.9 μm) appeared to be significantly greater than the laser treatments with either the low (9.7 ± 1.5 μm) or medium (8.0 ± 4.6 μm) fluences.

Generally, PSR-treated swine skin (Fig. 5) with a single pass using nozzle 2 did not produce a zone of thermal damage greater than 11 μm. In fact, 1.0 J did not produce any visible zone of thermal damage. Like the single pass with nozzle 2, the zone of thermal damage from a single pass with the standard nozzle (nozzle 1) did not exceed 11 μm in thickness, except for at 4.0 J (13 μm). The amount of thermal damage produced with either single pass or double pass using the standard nozzle was approximately the same. The only exception is in the case of 2.0 J (21 μm) in which the double pass with the standard nozzle produced more than twice the thermal damage compared to its equivalent single pass (9 μm).

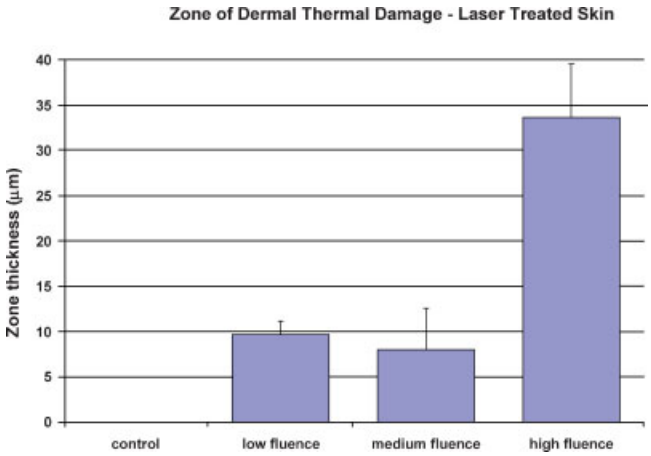

Fig. 4. The zone of thermal damage for low, medium, and high fluence laser-treated swine skin. Histograms represent the average of three treatments ± standard deviation.

Epidermal Necrosis and Intact Epidermis Post-Treatment

Epidermal necrosis was almost absent in the lowest PSR energy immediately post-treatment. The amount of epidermal necrosis was similar for low and medium laser and medium PSR energies, with the laser-treated sites demonstrating slightly more necrosis. The degree of necrosis did

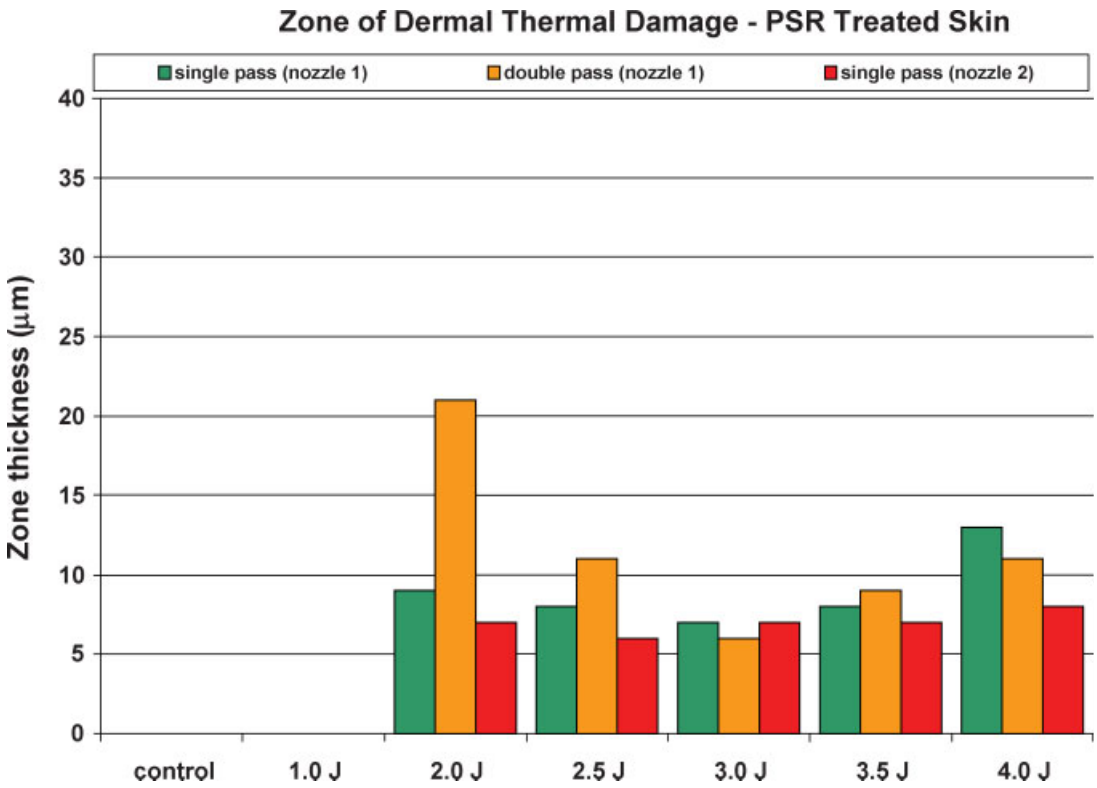

Fig. 5. Zone of thermal damage using 1.0, 2.0, 2.5, 3.0, 3.5, 4.0 J of PSR. Histograms represent single sample evaluations.

TABLE 2. Degree of Epidermal Necrosis and Percentage of Intact Epidermis at Each Biopsy Time-Point

Rx conditions	Day 0 Nec	Day 0	Day 2	Day 7	Day 14	Day 30	Day 60
Control	0	100	100	100	100	100	100
Laser low	3.1	41	41	100	100	100	100
Laser med	3.3	33	17	100	100	100	100
Laser high	4.7	7	17	100	100	100	100
PSR 1 J	0.3	94	100	100	100	100	100
PSR 2 J	3.4	32	59	100	100	100	100
PSR 2.5 J	2.9	43	88	100	100	100	100
PSR 3 J	2.9	43	18	73	100	100	100
PSR 3.5 J	2.9	45	46	100	100	100	100
PSE 4 J	3.1	38	15	100	100	100	100

not increase significantly with PSR going from 2–4 J, and stayed relatively constant, while almost complete epidermal necrosis was seen when using the highest laser energy (Table 2). Comparing laser and PSR for the amount of intact epidermis present post-treatment, PSR-treated skin had more intact epidermis at day 0 and day 2, comparing low, medium, and high treatment energies (Table 2). With the exception of a single biopsy specimen for 3.0 J of PSR, all biopsies demonstrated a fully intact epidermis for both laser and PSR by 7 days post-treatment, with epidermal recovery noted as early as day 2 in some specimens (Fig. 6).

Inflammation

Initially, inflammation could be observed in all laser-treated swine skin samples. Both low and medium fluences showed a general declining trend throughout the time points. By day 7, the inflammation from these treatments was at or below untreated control levels. Comparing the PSR treatments from a double pass (nozzle 1) to that of a single pass (nozzle 1), the inflammation appeared to decrease from day 0 to day 2. The exception to this was seen after the PSR treatment with 3.0 J. For PSR, inflammation decreased to baseline levels by 14 days post-treatment. In some cases, this occurred as of on day 7. It appeared that by day 2, a single pass with nozzle 2 stimulated more inflammation than a single pass with nozzle 1. However, by day 7, the inflammation produced by both single passes was below the control level of inflammation (Table 3).

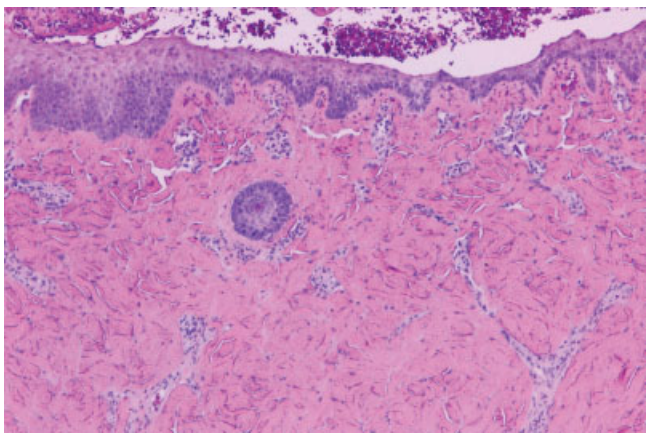

Fig. 6. Epidermal recovery of PSR-treated swine skin after 2 days. (2 J, single pass, nozzle 2). Note the formation of rête ridges.

DISCUSSION

The results of the study provided new data on the Plasma Skin Regeneration device. The PSR treatment left a zone of thermal damage equivalent to the low and medium fluence carbon dioxide laser treatments. High fluence laser treatment produced a zone of thermal damage of greater thickness than any energy of PSR used, including the use of two passes of PSR. The average ZTD for high fluence laser treatment in this study was somewhat higher (33.4 μm) than that noticed in previous studies performed on human abdominal skin using the UltraPulse 5000C (23.6 μm ± 2.5 μm at 300 mJ) [5]. This may be due to differences in water content between porcine and human skin, or to the energy density used in this study. Second passes with PSR only produced increased thermal damage on a single specimen, probably due to the insulating properties of the damaged tissue that was not wiped-off after the first pass.

TABLE 3. Inflammation Scores at Each Biopsy Time-Point

Rx conditions	Day 0	Day 2	Day 7	Day 14	Day 30	Day 60
Control	0.0	0.0	2.3	1.3	1.7	0.7
Laser low	2.1	1.3	1.0	1.0	1.3	0.0
Laser med	3.7	2.0	1.7	.0.7	0.7	0.3
Laser high	3.2	1.7	2.3	1.0	3.0	0.7
PSR 1 J	1.1	1.0	1.3	0.7	1.0	0
PSR 2 J	3.1	1.3	2.0	1.0	1.3	0
PSR 2.5 J	2.5	1.7	1.7	1.0	1.3	0.7
PSR 3 J	2.6	2.7	2.3	1.0	1.0	0.3
PSR 3.5 J	2.6	1.7	2.7	1.0	1.3	0.3
PSE 4 J	2.3	7.3	2.0	0.7	1.3	0

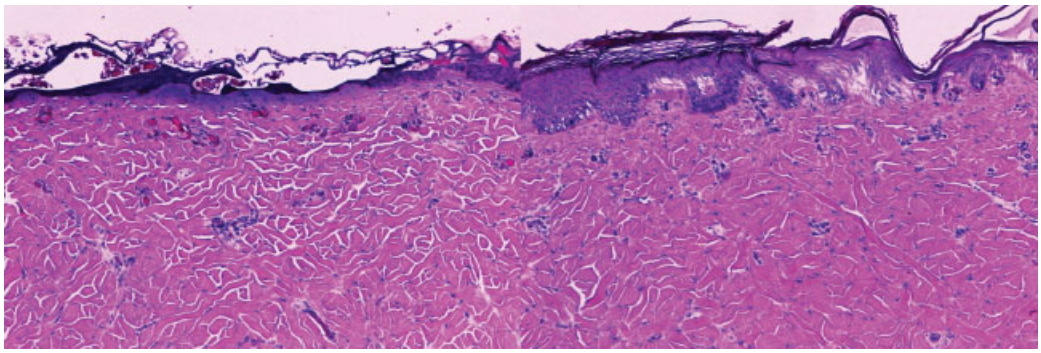

Fig. 7. High fluence CO_2 (**left**) and high energy PSR (4 J, **right**), immediately post-treatment.

It appears treatment with PSR produces a minimal zone of thermal damage. This is desirable since it can limit the amount of tissue damage and side-effects following treatment. A zone of thermal damage as seen here with PSR may be desirable to maintain hemostasis. Too narrow a zone of thermal damage, as can be seen following Er:YAG treatment, may limit the ability to ablate the dermis due to a lack of hemostasis.

As expected, epidermal necrosis increased with increasing fluence in the laser-treated skin. The amount of epidermal necrosis seen following PSR treatment at 1 J produced less epidermal damage than the lowest laser fluence. PSR treatment at 2 J had a similar amount of thermal damage to the lowest laser fluence. Two passes of PSR produced damage similar to the high laser fluence. PSR treatment at 3 J produced damage similar to the medium laser fluence, while 4 J produced damage between the medium and high laser fluences. Two passes of PSR at 3 and 4 J produced less damage than a single pass of PSR. Also of note, nozzle #2 produced less damage for a single pass at the same energy than nozzle #1. These results may speak to an insulating effect of the damaged tissue that was not wiped away, but too many conclusions cannot be drawn from a small sample size. However, it would appear that PSR can be used to produce less or similar damage to the laser fluences used here (Fig. 7).

With regard to the inflammatory response, the least amount of inflammation was observed in the low fluence group for laser-treated skin, with very similar results for medium and high laser fluences at days 0 and 2, and approximately baseline by day 7. PSR-treated skin demonstrated less inflammation than the lowest laser treatment energy on days 0 and 2 for energy of 1 J. With 2 J, inflammation was similar to the high and medium laser treatment groups, with little difference between 1 and 2 passes. At 4 J of PSR energy, the inflammation was similar to the high laser energy at day 0 and the low laser energy at day 2. With 2 J of PSR energy, inflammation was similar to the medium and high laser energies, but epidermal healing was faster than even the low fluence laser treatment. If inflammation correlates with clinical improvement, then it may be possible to get improved clinical results with faster healing. These conclusions cannot be drawn from the current study due to the small sample size and the inability to determine clinical improvement on photo-damaged human skin. A clinical study will be required to validate the results found to date.

The most unique histopathological finding following plasma skin resurfacing and in contrast to ablative laser treatment is the fact that the treated epidermis stays intact for a number of days until a new epidermis forms beneath it. It is only then that the treated epidermis sloughs off. This sequence of events results in a unique healing environment with the damaged epidermis serving as a physiologically "normal" dressing while the healing process takes place. This may result in qualitatively different effects of PSR as compared to other treatment modalities.

GENERAL CONCLUSIONS

Plasma skin regeneration treatment is capable of producing tissue effects similar to that seen with carbon dioxide laser treatment. Of interest is the increased rate of healing with the lower energy PSR groups. In addition, significant inflammation can be seen with even low PSR energies, possibly indicating the ability to produce a significant clinical effect with a quick healing time. Also of note is the confinement of thermal damage following single pass, high energy PSR treatment to less than 15 μm. This is desirable since it can limit the amount of tissue damage and side-effects following treatment, and could potentially result in the shedding of dyschromia, actinic keratoses, and superficial solar elastosis in the clinical setting. Future studies on sun-damaged facial skin will enable evaluation of the extent of clinical effect and correlate this with the rapidity of healing. This treatment is a different modality than laser, and thus may have significantly different clinical results. Future studies should be able to answer the questions raised here.

REFERENCES

1. Ross E, McKinlay JR, Anderson RR. Arch Dermatol 1999;135: 444–454.
2. Olhoffer I, Leffell D. Aesthet Dermatol Cosmet Surg 1999; 1:31–33.
3. Carniol PJ (editor). Laser skin rejuvenation. vol. 5. Philadelphia, PA: Lippincott-Raven; 1998. p 103–104.
4. Alster TS (editor). Cutaneous laser techniques. vol. 8. Lippincott Williams & Wilkins; 2000. p 119–120.
5. Bernstein E, Brown DB, Kenker J, Burns AJ. Dermatol Surg 1999;25(10):739–744.